URSI AP-RASC 2019, New Delhi, India, 09 - 15 March 2019

A 0.33-0.73 THz source based on phase-locked Josephson flux-flow oscillator

Nickolay V. Kinev* [(1)], Kirill I. Rudakov[(1),(2),(3)], Lyudmila V. Filippenko[(1)], Andrey M. Baryshev[(3)] and Valery P. Koshelets[(1)]
(1) Kotel'nikov Institute of Radio Engineering and Electronics of RAS, Moscow 125009, Russia, http://cplire.ru/
(2) Moscow Institute of Physics and Technology, Dolgoprudny 141701, Russia
(3) University of Groningen, 9712 CP Groningen, Netherlands

Abstract

A new implementation for a terahertz flux-flow oscillator (FFO) based on a long Josephson junction is presented. The oscillator is integrated with the lens antenna on a single chip providing the THz emission in the open space, and with a harmonic mixer (HM) based on a SIS junction for a frequency and phase locking. We used the double slot antenna to output the emission from the planar transmission line to the open space, this antenna is coupled to the elliptical silicon lens forming narrow output beam of THz radiation. Two designs of antenna and matching structures coupled to the oscillator are developed and fabricated, the operating ranges 0.33 - 0.57 THz and 0.42 - 0.73 THz were obtained experimentally for these designs. The emission to open space was measured by an external superconducting receiver located in the separate cryogenic system.

1. Introduction

An important problem nowadays in astronomy, spectroscopy, radio physics and other fields is the lack of easy tunable wideband THz sources. The FFO based on a long Josephson tunnel junction made of trilayers Nb-AlN-NbN or Nb-AlOx-Nb was successfully implemented as the local on-chip oscillator in the superconducting integrated receiver [1,2] and proved to be a perspective solution for an easily tuned and wideband source. It's operating bandwidth is about 100% of central frequency: from 250 GHz to 700 GHz for the sample having the length of 400 μm^2 and the width of 16 μm^2, and the free-running spectral linewidth is about several MHz with Lorentzian shape [3,4]. The upper operating frequency can potentially reach 1.2 THz if NbTiN-based output transmission lines are used [5]. Typically the phase locking loop (PLL) is used for such oscillator, for this purpose a small part of the output power is branched to the HM based on a SIS Josephson junction. The phase locking leads to an actual linewidth less than 100 kHz, which satisfy almost all needs for THz applications. The typical power of FFO is about 0.1 – 1 μW and can be increased by using larger current density of the Josephson junction.

2. Layout & numerical simulations

The output frequency f of the FFO is strictly defined by the Josephson equation $hf = 2eV_{DC}$, where V_{DC} is the DC voltage on the junction. The operation of such oscillator is discussed elsewhere [1,6]; the bias current and the control line current for supplying the local magnetic field are used for setting V_{DC} and hence the operation frequency f. The layout of the proposed oscillator based on the FFO is shown in fig. 1. The main idea of this work is the integration of the FFO with the HM for the feedback locking loop and with a transmitting slot antenna on a single microchip (fig. 1a) placed on the back surface of the elliptical lens (fig. 1b). The chip substrate and the lens are both made of silicon. Both tunnel junctions the FFO and the HM are to be fabricated of Nb/AlN/NbN or Nb/AlOx/Nb, top and bottom electrodes constitute the microstrip transmission lines. A similar type of slot lens antenna was used in [7] as the receiving antenna coupled to a SIS detector in the receiver for 100 GHz, 246 GHz and 500 GHz.

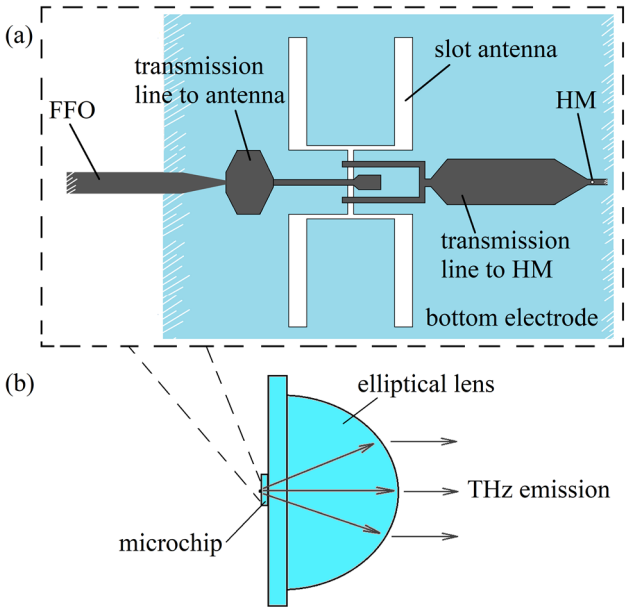

Figure 1. (a) Layout of the planar microcircuit containing FFO, double slot antenna, harmonic mixer and the coupling structures between the elements. (b) Scheme of the microchip with oscillator and antenna shown on (a) placed at the far focus of the silicon lens.

The numerical simulations of microcircuits shown in fig. 1a were carried out for different frequency ranges. The bandwidth of such antenna is about 0.4 - 0.5 of central frequency while the bandwidth of the FFO is up to ~1 of central frequency. Hence we decided to develop two designs to overlap 0.4 – 0.7 THz, with the central frequencies of 450 GHz (lower band design) and 600 GHz (upper band design). The numerical task is the coupling of the oscillator having low output impedance (less than 1 Ω) to the lens antenna having high impedance (tens of Ω) and forming a beam pattern required for applications, and simultaneous coupling to the HM having some intermediate impedance (about several Ω). Coupling to the antenna should be as high as possible, while coupling to the HM should be just enough for properly PLL operation (commonly 10-20 %) and should not take away much power. Both couplings with the antenna and the HM should be in the same frequency range, which is desired to be as wide as possible. The calculated impedances of two antenna designs are presented in fig. 2 a, and the calculated frequency properties of the whole microcircuits are shown in fig. 2b.

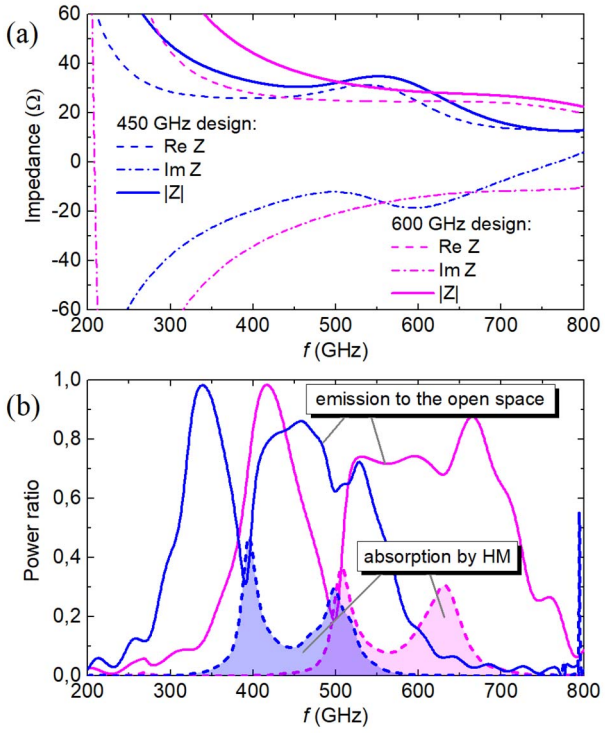

Figure 2. (a) The impedances of the slot antenna of 450 GHz and 600 GHz designs in the point of connection to a microstrip line. (b) The emission power to the open space (solid curves) and the absorption by the HM (dash curves with filling) for 450 GHz design (blue curves) and for 600 GHz (magenta curves). The power is normalized to the total output FFO power. The area under the dash curves are filled for clarity.

The simulations were carried out using the three-dimensional microwave modeling software. The emitting edge of the FFO was simulated as the input port #1 with the constant impedance of 0.5 Ω, the HM was simulated as a port #2 with the impedance equaled to the normal resistance of the junction. This resistance is about 20 Ω and defined by the current density of a real trilayer (typically 5 – 10 kA/cm^2) and the area of the junction, which is expected to be 1 - 1.5 μm^2. The capacity of the HM was taken into account by embedding a capacitor in parallel to the port #2 according to specific capacitance 85 fF/μm^2. The mictrostrip line behind the HM contains the rf-short in the form of radial stub to prevent the leakage of THz power beyond the HM. Then the microstrip line transforms to a CPW line for proper connection to the contact pads of the chip.

One can see from fig. 2a that the frequency dependence of the impedance for both designs is rather flat: the full impedance is found to change from 30 Ω to 40 Ω for 450 GHz design and from 26 Ω to 40 Ω for 600 GHz design. No jumps in the operation region are presented. According to results in fig. 2b, the operating ranges defined as the ranges with emission level to the open space higher than 0.7 of total FFO power are 330 – 550 GHz for lower band design and 400 – 700 GHz for upper band design. The power absorbed by the HM of about 0.1 - 0.2 was achieved in the regions of operation for both designs; which is expected to be enough for locking the oscillator.

3. Experiment

3.1 Setup

The DC measurements for Nb- and NbN-based structures are carried out by the dipstick testing in the liquid helium. The experimental setup for studying the output THz emission is shown in fig. 3; for this purpose the high resolution spectrometer based on the superconducting integrated receiver (SIR) [1,2] was used. Two liquid helium cryostats for the oscillator (upper part of the scheme in fig. 3) and the receiver (lower part of the scheme in fig. 3) were used and set opposite each other, so that the quasioptical windows of the cryostats were oriented toward one another. One can note that two FFOs are used in the experimental setup: one (FFO #1) is the object of the study, second one (FFO #2) is used as the local oscillator (LO) of the SIR. The local oscillator of 19 – 21 GHz is used for the mixing by the HM of the FFO signal and the n-th harmonics of the oscillator. Additionally, the PLL system is used for locking the signal. The spectral line of the emission can be measured simultaneously by the spectrum analyzer (SA) #1 in the intermediate frequency (IF) range of the HM 0 - 800 MHz, and by the SA #2 in the IF range of the SIR 4 – 8 GHz. Hence, the spectra detected by SA #1 is the convolution of the FFO #1 signal and the n-th harmonics of the synthesizer (assumed to be δ-function) while the spectra detected by SA #2 is the convolution of the two FFO signals, at least one of which (#2) should be phase-locked during the measurements forming the signal similar to δ-function.

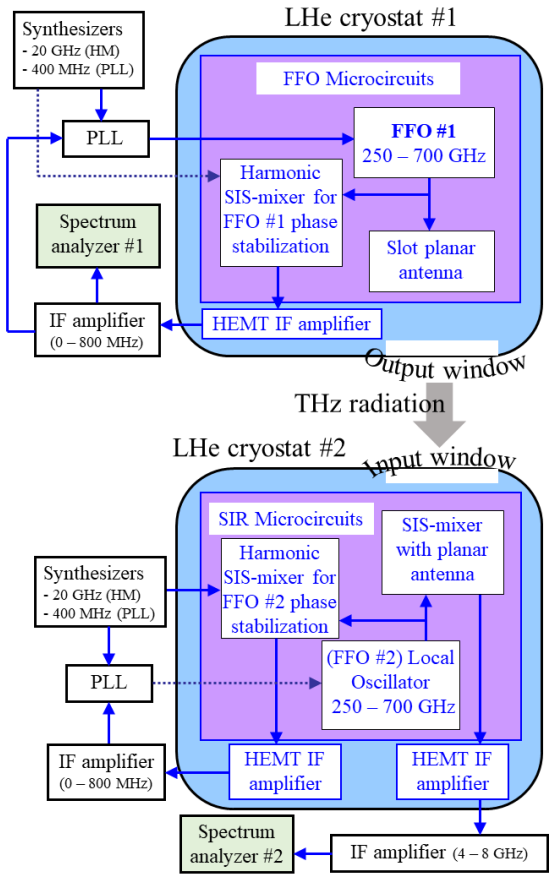

Figure 3. Block diagram of the experimental setup for measurements of the FFO emission to the open space by the THz spectrometer based on the SIR.

3.2. Results & discussion

The batch of experimental samples based on Nb/AlN/NbN tunnel trilayers was fabricated according to the developed 450 GHz and 600 GHz designs. The current density of the SIS trilayes on the batch is about $j_c = 11\text{kA/cm}^2$, this corresponds to parameter R_nS of about 19 $\Omega\cdot\mu\text{m}^2$; the gap voltage V_g is about 3.5 mV, and the quality factor of the HM junctions defined as the ratio of "sub-gap" resistance to normal resistance R_j/R_n is more than 25.

The pumping efficiency of the HM by the FFO was measured as the quasiparticle step on the current-voltage characteristics of the HM in the whole operating range of the FFO. The step is normalized to the "current jump" at V_g voltage, which is about 200 μA and is measured accurately for the specific junction. The results for the HM pumping in comparison with the calculation results are presented in fig. 4. One can note a good agreement of the experiment with the numerical simulations.

The output emission of the oscillators of both designs was successfully detected by the SIR in the ranges that were expected according to the numerical simulations. The typical spectral lines of the FFO at $f = 550$ GHz measured by the SA #1 (HM circuit) and by the SA #2 (SIR circuit) are presented in fig. 5. The Lorentzian shape of the free-running spectra are similar to each other, the estimated linewidth values are close. The detected power level is quite different due to different amplifications in the IF chains of the HM circuit and SIR output circuit (see fig. 3), so these power levels are incorrect to compare.

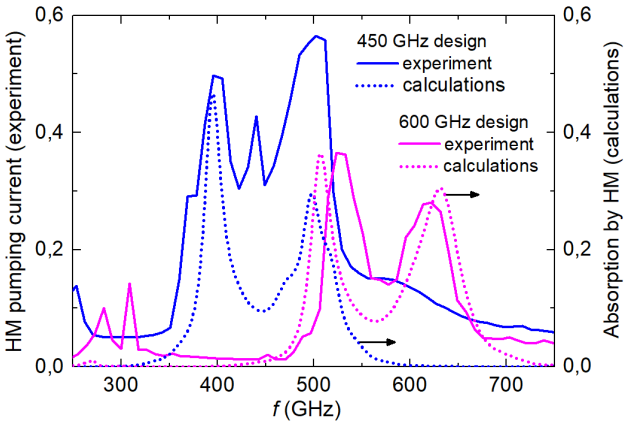

Figure 4. HM pumping by FFO power (solid curves) measured experimentally and calculation results of the absorbed FFO power by HM (dot curves). The HM pumping current is normalized to the "current jump" at the gap SIS voltage; the absorbed power is normalized to the total output FFO power. The dot curves are the same as the dash curves in fig. 2 b.

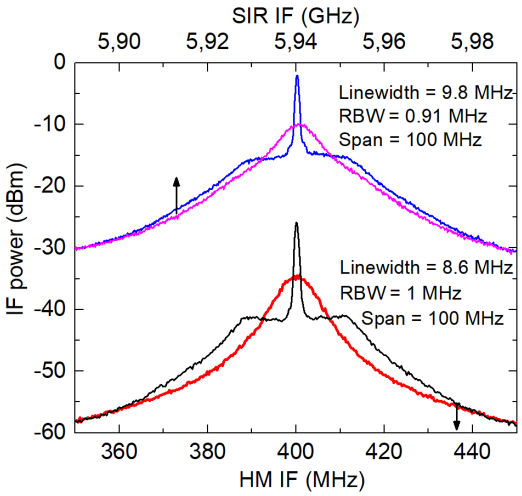

Figure 5. Power spectra of the FFO at the frequency 550 GHz for the sample of upper band design measured by using the on-chip HM (SA #1) – free-funning (red line) and phase-locked spectrum (black line), and by using the SIR (SA #2) – free-running (magenta line) and phase-locked spectrum (blue line). The bottom and top axes of frequency represent different IF ranges of output circuits, the span for both axes is the same and equals to 100 MHz. All the spectra are measured in the upper sideband. An estimated linewidth for free-funning spectra and the resolution bandwidth (RBW) of analyzers are shown near the curves. For the spectra measured by SIR (magenta and blue lines) the LO of the SIR, FFO #2, is phase-locked.

The emission to the open space of oscillator of both designs were studied in the range of SIR operation, as well as the signal branched to the feedback loop with the HM and PLL system; the results are presented in fig. 6. Since the range of SIR operation is about 450 – 700 GHz, which does not cover the wideband operating ranges of two designs, the emission at *f* lower than 450 GHz and higher than 700 GHz could not be measured accurately by the SIR. Nevertheless, these points still could be studied by the HM circuit to know the spectral properties. For studying the FFO emission to the open space at frequencies out of the SIR operation range another detector is required, e.g. Goley cell or a Si bolometer. Such experiment is planned for future.

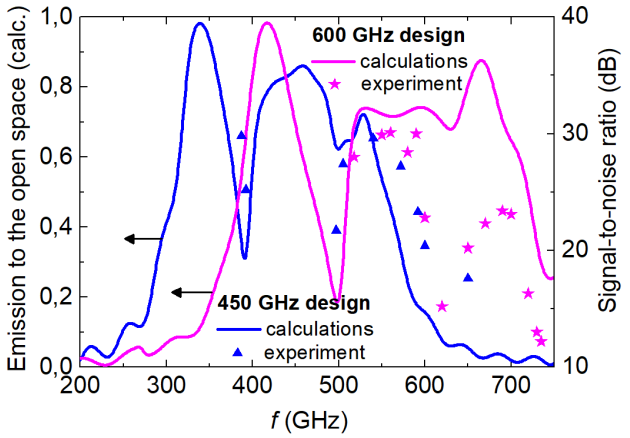

Figure 6. The signal-to-noise ratio detected by SIR in consequence of the FFO emission to the open space (scatter points) and calculation results (solid curves) for lower band and upper band designs. The solid curves are the same as the solid curves in fig. 2 b.

4. Conclusion

The superconducting THz oscillator based on a unidirectional flow of the fluxons in a long Josephson junction (a flux-flow oscillator or a FFO) is a promising solution of the THz source for the tasks where wideband frequency tuning is required and the high power is not necessary. We presented the implementation for the external THz source based on the FFO integrated with the harmonic mixer and the transmitting slot antenna integrated on a single chip with the oscillator. The lens is used forming the narrow beam pattern. Two antenna designs that covers 0.33 - 0.73 THz region are numerically simulated, fabricated and experimentally studied. The calculations are in a good agreement with the experiment. The emission to open space is measured by external high-resolution spectrometer, signal-to-noise ratio up to 30 dB is obtained with the free-funning spectral linewidth of about several MHz.

5. Acknowledgements

The development, fabrication and experimental measurements of the samples are supported by the Russian Science Foundation (project 17-79-20343). The development of the cryostats of experimental setup in Sec. 3.1 is supported by the RFBF (project 17-52-12051).

6. References

1. V. P. Koshelets, S. V. Shitov, "Integrated Superconducting Receivers," *Superconductor Science and Technology*, **13**, 5, December 2000, pp. R53-R69, doi:10.1088/0953-2048/13/5/201.

2. G. Lange, D. Boersma, J. Dercksen, P. Dmitriev, A. B. Ermakov, L. V. Filippenko, H. Golstein, R. Hoogeveen, L. de Jong, A. V. Khudchenko, N. V. Kinev, O. S. Kiselev, B. Kuik, A. de Lange, J. Rantwijk, A. S. Sobolev, M. Yu. Torgashin, E. Vries, P. A. Yagoubov, and V. P. Koshelets, "Development and Characterization of the Superconducting Integrated Receiver Channel of the TELIS Atmospheric Sounder," *Superconductor Science and Technology*, **23**, 4, March 2010, pp. 045016-1-045016-8, doi:10.1088/0953-2048/23/4/045016.

3. V. P. Koshelets, P. N. Dmitriev, A. S. Sobolev, A. L. Pankratov, V. V. Khodos, V. L. Vaks, A. M. Baryshev, P. R. Wesselius, and J. Mygind, "Line width of Josephson flux flow oscillators," *Physica C*, **372-376**, 1, August 2002, pp. 316-321, doi:10.1016/S0921-4534(02)00659-7.

4. V. P. Koshelets, S. V. Shitov, P. N. Dmitriev, A. B. Ermakov, L. V. Filippenko, V. V. Khodos, V. L. Vaks, A. M. Baryshev, P. R. Wesselius, and J. Mygind, "Towards a phase-locked superconducting integrated receiver: prospects and limitations," *Physica C*, **367**, 1-4, February 2002, pp. 249-255, doi:10.1016/S0921-4534(01)01046-2.

5. J. Kawamura, J. Chen, D. Miller, J. Kooi, J. Zmuidzinas, B. Bumble, H. G. Leduc, and J. A. Stern, "Low-noise submillimeter-wave NbTiN superconducting tunnel junction mixers," *Applied Physics Letters*, **75**, 25, December 1999, pp. 4013-4015, doi:10.1063/1.125522.

6. T. Nagatsuma, K. Enpuku, F. Irie, and K. Yoshida, "Flux-flow type Josephson oscillator for millimeter and submillimeter wave region," *Journal of Applied Physics*, **54**, 6, February 1983, pp. 3302-3309, doi:10.1063/1.332443.

7. D. F. Filipovic, S. S. Gearhart, and G. M. Rebeiz, "Double-slot antennas on extended hemispherical and elliptical silicon dielectric lenses," *IEEE Transactions on Microwave Theory and Techniques*, **41**, 10, October 1993, pp. 1738-1749, doi:10.1109/22.247919.